Journal of Molecular Evolution (2018) 86:618–634
https://doi.org/10.1007/s00239-018-9870-8

ORIGINAL ARTICLE

Evolutionary Genetics of Hypoxia and Cold Tolerance in Mammals

Kangli Zhu[1] · Deyan Ge[1] · Zhixin Wen[1] · Lin Xia[1] · Qisen Yang[1]

Received: 7 May 2018 / Accepted: 3 October 2018 / Published online: 16 October 2018

Abstract

Low oxygen and fluctuant ambient temperature pose serious challenges to mammalian survival. Physiological adaptations in mammals to hypoxia and low temperatures have been intensively investigated, yet their underlying molecular mechanisms need further exploration. Independent invasions of high-altitude plateaus, subterranean burrows and marine environments by different mammals provide opportunities to conduct such analyses. Here, we focused on six genes in the hypoxia inducible factor (HIF) pathway and two non-shivering thermogenesis (NST)-related genes [PPAR co-activator 1 (*PGC-1*) and uncoupling protein 1 (*UCP1*)] in representative species of pikas and other mammals to understand whether these loci were targeted by natural selection during independent invasions to conditions characterized by hypoxia and temperature fluctuations by high-altitude, subterranean and marine mammals. Our analyses revealed pervasive positive selection signals in the HIF pathway genes of mammals occupying high-altitude, subterranean and aquatic ecosystems; however, the mechanisms underlying their independent adaptations to hypoxic environments varied by taxa, since different genes were positively selected in each taxon and expression levels of individual genes varied among species. Additionally, parallel amino acid substitutions were also detected in hypoxia-tolerant mammals, indicating that convergent evolution may play a role in their independent adaptations to hypoxic environments. However, divergent evolutionary histories of NST-related genes were noted, since significant evidence of positive selection was observed in *PGC-1* and *UCP1* in high-altitude species and subterranean rodents; however, *UCP1* may have already lost its function in diving cetaceans, which may be related to the thick blubber layer of adipose and connective tissue in these mammals.

Keywords Hypoxia · Low temperature · Adaptive evolution · HIF pathway · NST · Differential expression

Introduction

Environmental stress has been a major driving force in the evolution of living organisms (Parsons 2005). Organisms may evolve similar survival traits when they face the same ecological stressors, thus providing an opportunity for biologists to study the basis of adaptive evolution and predict the repeatability of evolution (Gompel and Prud'homme 2009; Losos 2011; Stern and Orgogozo 2009; Storz 2016). Naturally occurring examples of convergent evolution are good choices for these studies. Independent invasions of high-altitude, subterranean and marine niches by pikas, subterranean mole rats and cetaceans, respectively, provide an excellent natural system to study the basis of adaptive evolution and convergent evolution of hypoxia adaptation and cold resistance.

As the highest plateau in the world, the Qinghai–Tibet Plateau (QHTP) has an average altitude of more than 4000 m and is characterized by hypoxia, low temperatures and strong UV radiation, which impose strong environmental stresses on resident animals. Pikas are small non-hibernating, diurnal lagomorphs that belong to the Ochotonidae family, and most species of this taxon are endemic to the QHTP and the Himalayas as well as their adjacent areas (Corbet 1978; Hoffmann 1993). A previous study also showed that the QHTP and its vicinity are the most likely ancestral range of extant pikas (Ge et al. 2012). Pikas have successfully evolved a series of physiological adaptations to survive in hypoxic conditions in high-altitude plateaus, including a blunted

Electronic supplementary material The online version of this article (https://doi.org/10.1007/s00239-018-9870-8) contains supplementary material, which is available to authorized users.

✉ Qisen Yang
yangqs@ioz.ac.cn

[1] Key Laboratory of Zoological Systematics and Evolution, Institute of Zoology, Chinese Academy of Sciences, Beijing, China

hypoxic pulmonary vasoconstrictive response (Ge et al. 1998), lower maximal heart rate (Pichon et al. 2013) and higher capillary density (Qi et al. 2008). In addition, physiological adjustments to cope with hypoxic environments can also be seen in diving cetaceans and subterranean rodents. Cetaceans are fully aquatic mammals that routinely breathe air at the surface and then submerge for several seconds to hours, whereas subterranean mole rats live in burrows characterized by low oxygen (O_2) concentrations and high carbon dioxide (CO_2) concentrations (Buffenstein 2000). Both cetaceans and subterranean mole rats have evolved increased blood O_2 carrying ability and modified circulatory and respiratory systems to meet their O_2 demands (Arieli et al. 1986; Johansen et al. 1976; Maina et al. 2001; Panneton 2013; Ramirez et al. 2007). Although physiological adaptations to hypoxic environments have been intensively investigated, examination of their underlying molecular mechanisms only began in recent decades.

In mammals, the HIF pathway plays crucial roles in the response to O_2 stress since it can induce the expression of genes involved in glucose metabolism, cell proliferation, erythropoiesis and vascularization (Maxwell 2005). Under normoxia, two proline residues in the O_2-dependent degradation domain (ODDD) and an asparagine residue located in the C-terminal transactivation domain (C-TAD) of HIFα are hydroxylated by prolyl hydroxylase domain proteins (PHDs) and factor inhibiting HIF-1 (FIH-1), leading to its degradation via the ubiquitin–proteasome pathway or preventing the binding of transcriptional co-activators, respectively (Masson and Ratcliffe 2014; Zhang et al. 2010); under hypoxia, HIFα will be stably expressed, form a heterodimer with HIF1β, and then induce the transcription of hypoxia responsive genes (Masson and Ratcliffe 2014). Prompted by the discovery of genes in the HIF pathway, the molecular mechanisms underlying hypoxia perception and adaptations have been studied in detail. In diving mammals, physiological studies on the HIF pathway in cetaceans revealed that the turnover rate and transcription activity of *HIF1A* are related to the diving behaviour of cetaceans (Bi et al. 2015). In addition, higher expression levels of *HIF1A* are observed in both subterranean *Spalax ehrenbergi* superspecies and pikas, which can be treated as adaptive strategies to cope with hypoxia (Li et al. 2009; Shams et al. 2004). Furthermore, genomic analyses of subterranean mole rats and domestic yak (*Bos grunniens*) endemic to the QHTP also revealed evidence of adaptation to hypoxic conditions that involved HIF1α target genes, p53 target genes, haemoglobin α, neuroglobin and others (Fang et al. 2014a, b; Qiu et al. 2012). Again, investigation of indigenous people living in the Tibetan Plateau also suggested that *HIF2A* and *PHD2* were top two positive selection candidates (Hu et al. 2017). In short, the HIF pathway has been investigated in different hypoxia-tolerant mammals, but most of these studies have focused on single genes, single groups or limited physiological levels.

The low temperatures on high-altitude plateaus and the high thermal conductivity and heat capacity of water challenge mammalian thermoregulatory systems, particularly for species living in cold water, such as the beluga whale (*Delphinapterus leucas*) (Citta et al. 2013; Kovacs et al. 2011). Pikas have evolved an unusually high resting metabolic rate and high NST (Li et al. 2001; Sheafor 2003) to ward off hypothermia, and cetaceans have a thick subcutaneous fat layer to store energy and stay warm (Dunkin et al. 2005; Struntz et al. 2004). In eutherian mammals, NST mainly occurs in brown adipose tissue (BAT), and to date, UCP1 is the only known protein expressed exclusively in BAT that controls NST (Bouillaud et al. 1986; Cannon and Nedergaard 2004; Jacobsson et al. 1985). UCP1, a mitochondrial inner-membrane protein, can generate heat by dissipating the proton gradient across the mitochondrial inner-membrane (Klingenberg and Huang 1999; Nicholls and Locke 1984). Indeed, mice lacking gene *UCP1* are sensitive to cold exposure (Enerbäck et al. 1997). For pikas living at high altitudes, their NST, cytochrome C oxidative activity and UCP1 content in BAT are significantly increased to defend against cold temperatures in winter (Wang et al. 2006), whereas the contribution of NST is lower in large mammals than in small eutherians (Cannon and Nedergaard 2004). Interestingly, genomic analysis in the bowhead whale (*Balaena mysticetus*) suggested that *UCP1* may have lost its function because of a stop codon in the C-terminal region (Keane et al. 2015). It will be interesting to explore whether the loss of *UCP1* is only restricted to the bowhead whale or has occurred in all cetaceans by adding more species and testing whether natural selection plays different roles in small and large mammals. In addition, *PGC-1*, a co-activator linked to NST, is also highly expressed in BAT and can be rapidly induced in BAT upon cold exposure in mice (Puigserver et al. 1998). A previous study showed that *PGC-1* can increase the expression of *UCP1* by co-activating the transcriptional factors assembled on *UCP1* (Lowell and Spiegelman 2000). However, molecular studies on *PGC-1* in mammals are still rare.

In this study, we chose representative species from high-altitude pikas to amplify *UCP1, PGC-1* and genes from the HIF pathway (including *HIF1A, HIF2A, HIF1B, PHD2, PHD3* and *FIH-1*). In combination with sequences downloaded from NCBI (https://www.ncbi.nlm.nih.gov/) and Ensembl (http://asia.ensembl.org/index.html), we aim to test the following: (1) which loci were targeted by natural selection during independent invasions to different hypoxic environments by high-altitude, subterranean and marine mammals; (2) whether molecular convergence played roles during their independent evolution processes; (3) whether *UCP1* has lost its function in all cetaceans and whether the evolutionary histories of *UCP1* and *PGC-1* are different

among small and large mammals; and (4) whether expression levels of individual genes differ between hypoxia-tolerant mammals and their phylogenetically related species.

Materials and Methods

Sample Collection, Polymerase Chain Reaction and DNA Sequencing

A total of eight *Ochotona* species occupying different high altitudes were collected in the field, and their detailed information is listed in Table S1, ESM. Genomic DNA was extracted from muscle tissues using a DNeasy Blood & Tissue Kit (TIANGEN) according to the manufacturer's instructions. The quality of extracted DNA samples was detected using agarose gels. Voucher specimens were preserved at the Institute of Zoology, Chinese Academy of Sciences. In addition, sequences of American pika (*Ochotona princeps*) were downloaded from Ensembl and used as references to design primers to amplify *UCP1, PGC-1* and genes in the HIF pathway (including *HIF1A, HIF2A, HIF1B, PHD2, PHD3* and *FIH-1*) in the eight pikas. The PCR primers are listed in Table S2, ESM. The PCR mixture (25 μL) contained 1 μL of DNA, 0.5 μL of each primer and 23 μL of PCR Mix (TSINGKE). We used touch down methods to perform PCR with the following cycling parameters: duration of 2 min at 98 °C, 3 cycles of 98 °C for 10 s, 57–60 °C for 10 s, 72 °C for 10 s, 3 cycles of 98 °C for 10 s, 55–58 °C for 10 s, 72 °C for 10 s, 30 cycles of 94 °C for 10 s, 52–55 °C for 10 s, 72 °C for 10 s, and finally, an elongation of 72 °C for 30 s. The amplified PCR products were verified with agarose gels and then sent to Tsingke biological technology company for sequencing. Each PCR product was sequenced from both directions using ABI PRISM 3730 DNA sequencers. Gene sequences of other mammals were downloaded from Ensembl and NCBI with the accession numbers listed in Table S3, ESM. Sequence alignments were performed by ClustalW (Thompson et al. 1994) in MEGA6 (Tamura et al. 2013). For each sequence alignment, we used the program Gblocks 0.91b with parameter b5 = with half (Castresana 2000) to eliminate poorly aligned positions and divergent regions, and then each of them was visually inspected again. All sequences except for pseudogenes were first translated into protein sequences and aligned and were then translated back into nucleotide sequences.

Analysis of Evolutionary Selective Pressure

The conventional program for selective pressure analyses is codeml in PAML v4.9d, which is a package of programs for phylogenetic analyses based on maximum likelihood (ML) (Yang 2007). Estimation of the non-synonymous and synonymous substitution ratio (ω) is indicative of natural selection acting on the protein. Simplistically, $\omega > 1$, $= 1$ and < 1 indicate positive selection, neutral evolution and negative selection, respectively. In our study, we divided the sequences into two datasets: pikas-only and all-mammals. The commonly accepted species trees for pikas and all mammals were used as the input trees in our analyses (Fig. S1, ESM) (Fang et al. 2014a, b; Ge et al. 2012; Lindblad-Toh et al. 2011; Zhou et al. 2011).

Since positive selection will not affect all sites and all lineages over a prolonged time, we chose different models in PAML to detect positive selection on specific sites and lineages. Here, M2a vs M1a, M8 vs M8a and M8 vs M7, which allow ω to vary among different sites, were used in site model to detect positively selected sites (PSSs) in the pikas-only and all-mammals datasets. Branch model (including free ratio and one ratio) was used to detect branches with positive selection signals, but a previous study showed that the free ratio is parameter rich and prone to inaccurate estimation (Yang et al. 2000). Therefore, in this study, we used the one ratio (which assumes that all branches across the tree have a single ω) and one ratio constrained (which fixes $\omega = 1$ across the phylogenetic tree) as suggested in Sunagar et al. (2012) to evaluate the selective pressure acting on all mammals. We used branch site model (Ma vs Ma1) that assumes a subset of site-selective pressures varying in the foreground lineage to observe positive selection on specific residues of specific lineages in the all-mammals datasets. Clade C and its null model M2a_rel were used to evaluate selective pressures affecting groups of related taxa in the all-mammals datasets. Clade C models were developed for all cetaceans, all high-altitude mammals (including all pikas, domestic yak and Tibetan antelope), all pikas, domestic yak plus Tibetan antelope and all subterranean rodents [including blind mole rat (*Spalax galili*), naked mole rat (*Heterocephalus glaber*) and Damaraland mole rat (*Fukomys damarensis*)]. In addition, for Clade C model, we also constructed datasets containing only one focal clade in order to avoid their influence on one another, i.e. datasets only containing cetaceans + outgroup (non-hypoxia-tolerant mammals), subterranean mole rats + outgroup, all pikas + outgroup, domestic yak plus Tibetan antelope + outgroup and high-altitude mammals + outgroup. The p values were estimated assuming a null-distribution that is a 50:50 mixture of a chi-squared distribution and a point mass at zero, and only genes with $p < 0.05$ were considered. Bayes empirical Bayes (BEB) sites with posterior probabilities > 0.90 of belonging to the "$\omega > 1$" class were treated as sites under positive selection (Yang 2005) in our analyses.

In contrast to methods implemented in PAML (Yang 2007), which only considers variation in the non-synonymous substitution rate, the ML-based methods implemented in Datamonkey (http://www.datamonkey.org/) incorporate

variation in both non-synonymous and synonymous substitution rates across sites (Kosakovsky Pond and Frost 2005a, b). Here, we used random effects likelihood (REL), fixed effects likelihood (FEL) and fast unconstrained Bayesian approximation (FUBAR) methods in Datamonkey to detect PSSs in both pikas-only and all-mammals datasets. REL has greater power to detect positive selection in datasets of intermediate size but suffers from high false-positive rates in datasets with few sequences; however, FEL is better at capturing rate variation and does not suffer from as many false positives in small datasets (Kosakovsky Pond and Frost 2005a, b). FUBAR, which was developed later, has sped up the detection of positive selection and relaxed REL restrictions (Murrell et al. 2013). In this study, sites with a significance level < 0.2 in FEL, Bayes factor > 50 for REL and posterior probability < 0.8 for FUBAR were treated as PSSs. Only sites identified by two ML methods were used for further analyses.

Some studies have shown that ML-based methods will produce false-positive results and provide less evidence about the cause of selection (Suzuki and Nei 2002, 2004); therefore, we used a complementary protein level method implemented in TreeSAAP to support the ML-based results in both pikas-only and all-mammals datasets (Woolley et al. 2003). TreeSAAP classifies the magnitudes of amino acid replacements in eight categories, measures the selective influences on 31 structural and biochemical amino acid properties during cladogenesis, and performs goodness-of-fit and categorical statistical tests (Woolley et al. 2003). In our analyses, only sites satisfying the following two criteria were treated as PSSs: (1) sites assigned to categories with radical functional or structural changes (i.e. categories 6–8), and (2) sites that were significant at $p < 0.05$.

Analysis of Pseudogenized *UCP1* in Cetaceans

For pseudogenes, we removed the premature stop codons and/or ORF-disrupting indels first, and then followed the procedures described in Zhao et al. (2010) to estimate ω using PAML v4.9d. We constructed five different models to infer the evolutionary history of cetaceans. First, we constructed model A (which allows a single ω value across the tree) and model B (which fixes the ω value across the tree to be 1) to evaluate the selective pressure affecting the whole phylogenetic tree. Second, to see whether cetaceans possessed a different ω value, we used model C which allowed different ω values between pseudogenized cetacean branches and the rest branches. To further investigate whether selective pressure have already completely removed in cetaceans, we constructed model D. Model D allowed selective pressure falling on the pseudogenized cetacean branches to be 1, and the rest branches had a different ω value. At last, we constructed model E, and this model assigned different ω values for each branch in the tree.

Convergent Evolution Analysis in Hypoxia-Tolerant Mammals

Similar environmental challenges may induce the evolution of phenotypic convergence between different species. Convergently evolved character states can result from convergent/parallel amino acid replacements [along different phylogenetic lineages, changes from different ancestral states to the same descendant amino acid are defined as convergent changes, whereas changes from the same ancestral state to the same descendant amino acid are defined as parallel changes (Zhang and Kumar 1997)], but to what extent a convergent phenotype is caused by convergent/parallel amino acid substitutions is a key question in evolutionary biology (Bridgham 2016; Natarajan et al. 2016; Stern 2013; Zhang and Kumar 1997). Here, we used different methods to detect the molecular basis of convergent hypoxic adaptation in high-altitude (pikas, domestic yak and Tibetan antelope), diving (cetaceans) and subterranean (subterranean mole rats) mammal groups.

In our study, we first constructed phylogenetic trees of six HIF pathway genes (*HIF1A, HIF2A, HIF1B, PHD2, PHD3* and *FIH-1*) using MrBayes 3.2 (Ronquist et al. 2012) to test whether hypoxia-tolerant mammals grouped together. JModelTest 2.1.7 was used to calculate the best-fit models of nucleotide substitution under the Akaike information criteria (Darriba et al. 2012; Guindon et al. 2003). For MrBayes inference, tree searches were run using four Markov chains for a minimum of 10 million generations and sampled every 1000 generations. A consensus tree was estimated after removing the first 1000 tree as burn-in.

Second, according to methods introduced in Zou and Zhang (2015), we computed the observed and expected number of convergent and parallel substitutions between each pair of hypoxia-tolerant mammals under neutral models termed Jones, Taylor and Thorton (JTT)-f_{site}, which has replaced the equilibrium amino acid frequencies in the JTT model with the observed amino acid frequencies at the site across all sequences in the alignment. Protein alignments for HIF pathway genes were analysed using codeml program in PAML v4.9d (Yang 2007). The Empirical + F model together with the JTT matrix was used, and a discrete gamma model with eight rate categories was used to calculate among-site rate variation. From the PAML output, we extracted the branch lengths of the tree, relative substitution rate of each site and inferred ancestral sequences.

In addition, we also extracted convergent/parallel and unique amino acid substitutions based on sequence alignments, since convergent phenotypic characteristics can also arise from unique substitutions that independently evolved in

different species (Natarajan et al. 2015; Stern 2013). In the all-mammals datasets, we performed sequence alignments with ClustalW (Thompson et al. 1994) in MEGA6 (Tamura et al. 2013), and chose convergent/parallel amino acid substitutions and those specific to each hypoxia-tolerant mammal group (including the high-altitude, diving and subterranean groups).

Structure Analysis

We investigated whether positively selected, convergent/parallel and group-specific residues affect protein function by mapping these sites onto three-dimensional protein structures. Protein structures were obtained from Protein Data Bank (http://www.rcsb.org/pdb/home/home.do), a database containing 3D shapes of proteins, nucleic acids and complex assemblies, or constructed by I-TASSER, a hierarchical approach for protein structure and function prediction (https://zhanglab.ccmb.med.umich.edu/I-TASSER/) (Zhang 2008). We used the PyMol (http://www.pymol.org) for visualization and structure mining.

Analysis of Differential Gene Expression

The expressions of *UCP1, PGC-1* and six HIF pathway genes (*HIF1A, HIF2A, HIF1B, PHD2, PHD3* and *FIH-1*) were examined in publicly available RNA-seq data. Here, we mainly focused on RNA-seq data from lung and heart, since previous studies showed that circulatory and respiratory systems in cetaceans and pikas have been modified to meet oxygen demand in low oxygen environments (Ge et al. 1998; Panneton 2013; Pichon et al. 2013; Ramirez et al. 2007). American pika samples collected from high (1400 m) and low (300 m) elevation sites were sequenced by 454 GS FLX Titanium platform, and five tissues (heart, liver, brain, gonad, liver) were sequenced with single-end layouts (Lemay et al. 2013) (Table S4, ESM). Common mink whale (*Balaenoptera acutorostrata*) (1 lung and 1 heart) (Yim et al. 2014), domestic yak (1 lung and 1 heart) (Qiu et al. 2012) and cow (*Bos taurus*) (2 lungs and 2 hearts) (Merkin et al. 2012) were sequenced by Illumina HiSeq 2000 platform, and all of them had paired-end library layouts (Table S4, ESM). Reference genome sequences were downloaded from NCBI (Table S5, ESM). FastQC (http://www.bioinformatics.bbsrc.ac.uk/projects/fastqc) was used to check read quality and raw reads in FASTQ format were filtered for adapter contamination, ambiguous residues (N's) and low-quality regions using Trimmomatic 0.36 (Bolger et al. 2014). For quality-based trimming, we used the quality filtering functionality of Trimmomatic with a sliding window, which will scan at the 5′ end and clip the read once the average quality within the window falls below 15. Then, we used two methods to conduct differential expression analyses, one based on RSEM: for each species, all the cleaned reads were mapped to the reference genome sequences with STAR v2.6.0c (Dobin et al. 2013), and then RSEM v1.3.0 was used to estimate and quantify the gene and isoform abundances (Li and Dewey 2011). The other method is based on TopHat2: for each species, TopHat2 v2.1.1 and Bowtie2 v2.2.3 were used for alignment (Langmead and Salzberg 2012; Kim et al. 2013), and read counting was performed by featureCounts (Liao et al. 2014). Finally, the R package edgeR was used to normalize the expression levels by Trimmed Mean of M-values (TMM) correction (Robinson et al. 2009; Robinson and Oshlack 2010). If the sequencing depth is reasonably consistent across the RNA samples (the ratio of the large library size to the small one is not more than about threefold), the normalized counts were subject to the simplest limma-trend approach with trend = TRUE for the eBayes function and correction for multiple testing (Benjamini–Hochberg false discovery rate of 0.05) (Law et al. 2014). When the library sizes are quite variable between samples (i.e. the ratio is greater than threefold), normalized read counts were next subjected to the voom function in limma R package with trend = TRUE for the eBayes function and correction for multiple testing (Benjamini–Hochberg false discovery rate of 0.05) (Law et al. 2014). Following limma analysis, we have set strict parameters to denote genes as differently expressed between pairwise comparisons among hypoxia-tolerant mammals and their partners: genes with a log2 fold-change of at least 2.0, a Benjamini–Hochberg-adjusted *p*-value less than or equal to 0.05 and a *B*-value of least 2.945 were defined as significant genes.

Results

Characterization of Amplification Results

In this study, we successfully amplified six HIF pathway genes (*HIF1A, HIF2A, HIF1B, PHD2, PHD3* and *FIH-1*), *UCP1* and *PGC-1* from representative *Ochotona* species (Table S6, ESM). Newly obtained sequences were deposited in GenBank with accession numbers MG811875-MG811938, reaching 55.61 (471 aa/847 aa in *HIF1B*) to 97.98% (778 aa/794 aa in *PGC-1*) of the coding regions according to the reference sequences from American pika. Based on the sequence alignment of each gene, we did not identify any premature stop codons or frame shift mutations in any of the amplified pika sequences, suggesting that all these genes may still be functional in pikas.

Detection of Signatures of Positive Selection and Differential Gene Expression Analysis

For the pikas-only datasets, we used site model (M2a vs M1a, M8 vs M8a and M8 vs M7) in PAML and FEL, REL and FUBAR methods in Datamonkey to detect PSSs in this high-altitude group. In total, we identified 13 PSSs detected

by at least two ML methods in five genes (including *HIF1B, PHD2, PHD3, PGC-1* and *UCP1*) (Table 1). As a complementary protein level approach to ML methods, TreeSAAP was applied to limit PPSs to those with effects on function or changes in amino acid properties. This retained nine of 13 PSSs in the above five genes. Furthermore, based on differential gene expression results from both TopHat2 and RSEM methods, we did not identify any genes up- or down-regulated in the American pikas from high elevation site when compared to those from lower site (Tables S7–S8, ESM).

In the all-mammals datasets, we used a series of methods to detect PSSs and positively selected lineages and to determine which loci were targeted by natural selection during mammalian invasions to environments with low O_2 and/or fluctuant ambient temperatures. First, we used the simplest branch model one ratio (which assigns all branches across the phylogenetic tree a single ω) vs one ratio constrained (which fixes $\omega = 1$ across the tree) to evaluate selective pressure affecting all mammals. Our results showed that for all genes, one ratio was better than its null model (p values all significantly less than 0.001) and ω values ranged from 0.026 to 0.199 (Table S9, ESM), suggesting that negative selection still played important roles.

Second, by combining the results from site model and Datamonkey, we identified 47 PSSs scattered among seven genes (including 23 sites in five HIF pathway genes: *HIF1A, HIF2A, HIF1B, PHD2* and *PHD3* and 24 sites in two NST-related genes: *UCP*1 and *PGC-1*) (Table 2). Further, TreeSAAP analyses reduced PSSs with radical amino acid changes to 21 in four genes (including nine sites in three HIF pathway genes: *HIF1A, HIF2A* and *PHD3*, and 12 sites in *PGC-1*) (Fig. 1; Table 2).

Third, branch site model was more powerful than the other models, and it may be a useful tool for detecting episodic positive selection and generating biological hypotheses for mutation studies and functional analyses (Yang and dos Reis 2011). In our study, positive selection signatures were only detected in *UCP1* and two HIF pathway genes (*HIF2A* and *PHD3*) (Fig. 1; Table 3), and different lineages and sites were affected. In *UCP1*, subterranean naked mole rat was under positive selection ($\omega 2 = 999.000$, $p = 0.028$). Moreover, in *HIF2A*, only high-altitude Tibetan antelope was positively selected ($\omega 2 = 999.000$, $p < 0.001$), and in *PHD3*, both diving and high-altitude mammals were positively selected (including American pika ($\omega 2 = 67.825$, $p = 0.007$) and common bottlenose dolphin (*Tursiops*

Table 1 Selective pressure analyses of genes in the HIF pathway and NST-related genes in the pikas-only datasets

Gene	Position	PAML		DataMonkey			TreeSAAP Properties		Functional domain
		Site model (M8)	Site model (M2a)	FEL $p < 0.2$	REL BF > 50	FUBAR pp > 0.8	Radical changes in AA properties[a]	Total	
HIF1B									
	306			0.189		0.892	*Pα*	1	
PHD2									
	143				8.722E+08	0.878	*Pα c*	2	
	176				7.472E+08	0.838			
PHD3									
	16			0.184	3068.790	0.839	*pK′ Ra* H_p	3	
	204	0.956*	0.960*		72282.900	0.888			
PGC-1									
	243	0.958*		0.182	553.565	0.900			
	326	0.958*		0.147	514.647	0.897	*Ns P*	2	NLS[b]
	364	0.977*		0.105	9473.830	0.967	*Pα P*	2	
	371	0.964*		0.131	566.831	0.911	*Pα*	1	
	423	0.957*		0.184	486.080	0.864	*Ns Br*	2	
	439	0.956*			454.106	0.864			
	714	0.955*			417.982	0.844	*Ns Br*	2	RNP[c]
UCP1									
	10			0.193	1426.250	0.845	H_t	1	

[a]Radical changes in amino acid properties under categories 6–8 were detected in TreeSAAP. Physicochemical amino acid properties are as follows: *Br* buriedness, *c* composition, H_p surrounding hydrophobicity, H_t Thermodyn transfer hydrophob., *Ns* Average # surrounding residues, *P* turn tendencies, *Pα α* – helical tendencies, *pK′* Equil. Const. – ioniza., COOH; *Ra* Solvent accessible reduct ratio

[b]Nuclear localization signal

[c]RNA-binding domain

Table 2 Selective pressure analyses of genes in the HIF pathway and NST-related genes in the all-mammals datasets

Gene	Position	PAML	DataMonkey			TreeSAAP properties				Functional domain
		Site model (M8)	FEL $P<0.2$	REL BF > 50	FUBAR pp > 0.8	AA changes	Clade	Radical changes in AA properties[a]	Total	
HIF1A										
	584	0.954*	0.072	628.298	0.908					ODDD/N-TAD[b]
	597	0.966*		360.704		Ile → Val	m1	pK'	1	
	598	0.978*		126.019						
	600		0.174	952.745	0.856	Ala → Thr	c1	$P\alpha$	1	
	602	0.945		72.633		Ala → Ile	e1	pK'	1	
						Thr → Ala	e	$P\alpha$	1	
	603		0.066	236.405	0.897					
	608	0.933		76.426		Gly → Glu	e	$P\alpha$	1	
	622		0.173	55.013						
	626		0.161	56.483						
	634	0.912		131.261						
	644	0.949		50.835						
	682		0.109	73.422		Val → Ile	o	pK'	1	
HIF1B										
	262		0.079		0.805					Near to PAS-A[c]
HIF2A										
	468		0.139	54.852		His → Glu	e	α_c	1	Near to ODDD/N-TAD
	653		0.058	122.073	0.868	Thr → Ile	l1	$H_p H_t$	2	
	682		0.036	153.276	0.872					
PHD2										
	252		0.164	155.433						
	253	0.906			0.824					
PHD3										
	9		0.118	78.911						
	16		0.055		0.881	Ile → Thr	e1	pK'	1	
						Val → Ile	g	pK'	1	
	53		0.095		0.847	Asn → Asp	l1	α_c	1	
	55		0.145	50.572						
	234		0.133	136.860						
UCP1										
	84			58.159	0.816					
	108			81.631	0.801					

Table 2 (continued)

Gene	Position	PAML	DataMonkey			TreeSAAP properties				Functional domain
		Site model (M8)	FEL $P<0.2$	REL BF > 50	FUBAR pp > 0.8	AA changes	Clade	Radical changes in AA properties[a]	Total	
PGC-1										
	102		0.175	214.616						NID1[d]
	205		0.170	68.692						NID2[e]
	208		0.181	67.863		Thr → Ala	l1	$P\alpha$	1	NID2
	224		0.012	671.841	0.980					NID2
	294		0.103	431.222		Ala → Thr	h	$P\alpha$		
	300		0.091	474.263						
	313		0.046	782.683	0.851	Ala → Thr	x1	$P\alpha$		NLS[f]
	318		0.020	671.541	0.958	Thr → Ala	e	$P\alpha$		
	343		0.092	469.614						
	399		0.121	83.133	0.925	Ser → Ala	e	$P\alpha$		
	402		0.199	76.729						
	403		0.136	338.984		Gly → Arg	e	$Mv\ M_w\ V^0\ \mu$		
	413		0.111	234.393						
	415		0.127	290.567		Tyr → Ser	f	V^0		
	416		0.085	103.090		Leu → Pro	q1	$P\alpha$		
	421		0.161	214.348		Glu → Gly	v	$P\alpha$		
	423		0.198	207.724						
	504		0.191	209.769						
	512		0.173	66.171		Ser → Ala	t1	$P\alpha$		
	634		0.116	285.628	0.810					NLS
	698		0.200	204.310		Ser → Cys	i1	μ		RNP[g]
	758		0.094	460.858		Thr → Ala	l1	$P\alpha$		

[a]Radical changes in amino acid properties under categories 6–8 were detected in TreeSAAP. Physicochemical amino acid properties are as follows: α_c Power to be—C-term., α-helix, H_p surrounding hydrophobicity, H_t Thermodynamic transfer hydrophob, Mv molecular volume, M_w molecular weight, $P\alpha$ α—helical tendencies, pK' Equil. Const. – ioniza., COOH; μ refractive index; V^0 partial specific volume

[b]Oxygen-dependent degradation and N-terminal transactivation domain

[c]PER ARNT SIM A domain

[d]Nuclear receptor interaction domain 1

[e]Nuclear receptor interaction domain 2

[f]Nuclear localization signal

[g]RNA binding domain

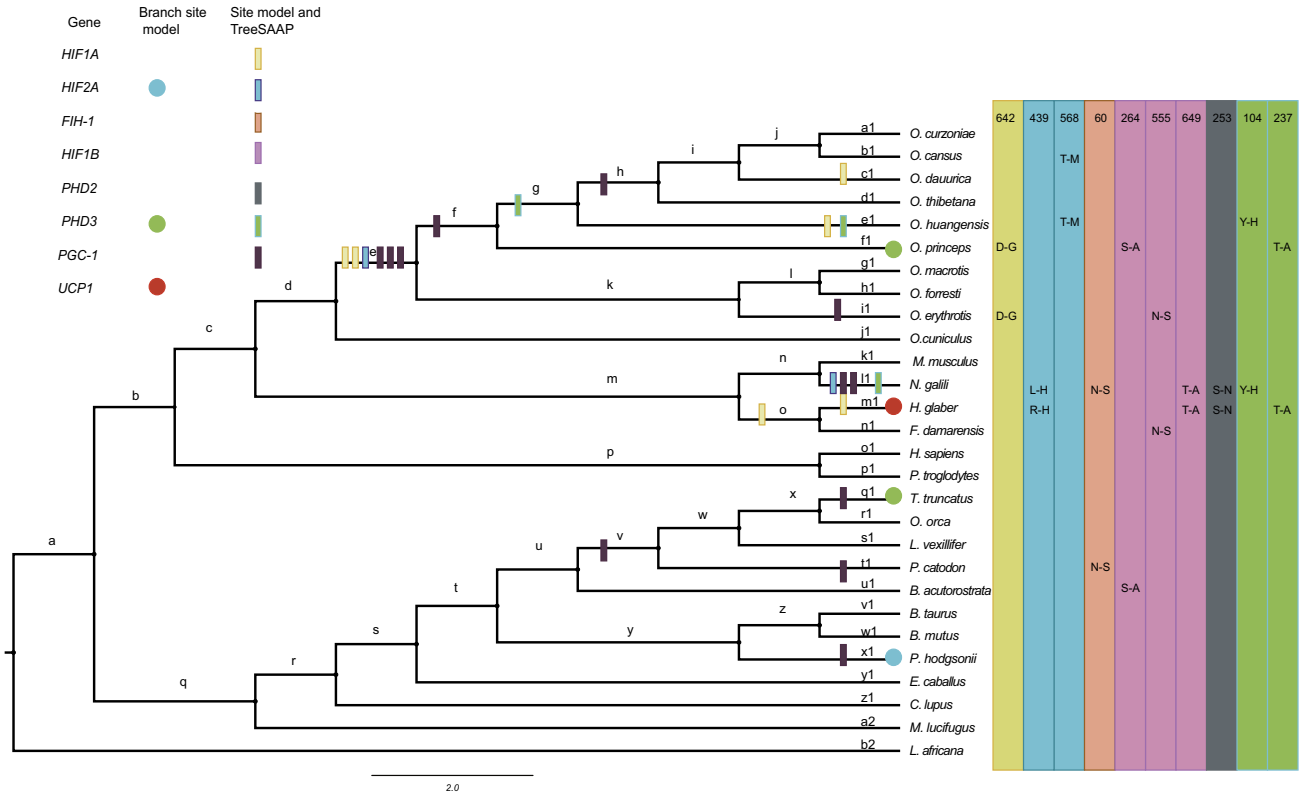

Fig. 1 Positive selection at *UCP1, PGC-1* and six HIF pathway genes across the phylogenetic tree. Radical amino acid changes of positively selected sites and positively selected branches of the corresponding gene were marked throughout the phylogenetic tree using boxes and circles of different colours, respectively. Parallel/convergent amino acid changes occurred in *HIF1A* (yellow), *HIF2A* (cycan), *FIH-1* (orange), *HIF1B* (purple), *PHD2* (grey) and *PHD3* (green) in the lineages listed to the right of the corresponding terminal branches. Amino acid positions (numbers) and parallel changes at each position are listed on the right side of Fig. 1

truncatus) ($\omega 2 = 645.215$, $p < 0.001$)). In favour of this result and according to results from Clade C model in the all-mammals datasets (Table 3), we found that the clade including all cetaceans was marginally positively selected in *PHD3* ($\omega 3 = 1.162$, $p = 0.053$), and in *HIF2A* ω value, falling on clade containing domestic yak and Tibetan antelope was significantly greater than its background lineages ($\omega 2 = 0.291$, $\omega 3 = 0.751$, $p = 0.007$). Moreover, in *PGC-1*, we detected positive selection signals falling on two focal clades that included all cetaceans ($\omega 3 = 1.554$, $p = 0.002$) and all pikas ($\omega 3 = 4.214$, $p = 0.007$). When considering datasets only with one focal clade, we obtained similar results (Table S10, ESM).

At last, using RNA-seq data from lung and heart in the diving common mink whale, high-altitude domestic yak and their closely related partner cow, we conducted a series of differential gene expression analyses to see whether expression levels of each gene were different among them. Combined TopHat2 and RSEM results, we only found expression of *PHD3* was up-regulated in the heart of domestic yak (Tables S7-S8, ESM).

Convergent Hypoxic Adaptation in Hypoxia-Tolerant Mammals

In our study, gene trees constructed by MrBayes did not group any hypoxia-tolerant mammal groups together for the six genes in the HIF pathway (Figs. S2–S7, ESM). In addition, based on comparisons between observed and expected number of convergent and parallel substitutions among each pair of hypoxia-tolerant mammals under JTT-f_{site} model, our results revealed eight pairs of hypoxia-tolerant mammals possessed higher-than-neutral substitutions, and five of them reached a significant level (Table S11, ESM). Based on sequence alignments, we found these five parallel sites scattered in four genes including *HIF1A, HIF2A, HIF1B* and *PHD3* (Table S12, ESM).

In addition to convergent/parallel amino acid substitutions, convergent phenotypic characteristics can also arise from unique substitutions (Natarajan et al. 2015; Stern 2013). Based on sequence alignments of six HIF pathway genes, a total of 14 unique substitutions were identified in diving cetaceans and subterranean rodents (including 11

Table 3 Selective pressure analyses by branch-site and Clade C models in the all-mammals datasets

Model	Gene	Model compared	2ΔLnL	*p*-value	*ω* values	Positively selected sites
Branch site	*HIF2A*					
		Branch (terminal branch of *Pantholops hodgsonii*)				
		Null	34.322	< 0.001	$\omega0=0.049$, $\omega1=1.000$, $\omega2=1.000$	
		Alternative			$\omega0=0.049$, $\omega1=1.000$, $\omega2=999.000$	187 T 0.997**;191 K 0.990*;193 Y 0.998**
	PHD3					
		Branch (terminal branch of *Ochotona princeps*)				
		Null	7.324	0.007	$\omega0=0.024$, $\omega1=1.000$, $\omega2=1.000$	
		Alternative			$\omega0=0.024$, $\omega1=1.000$, $\omega2=67.825$	205 * 0.920
		Branch (terminal branch of *Tursiops truncatus*)				
		Null	17.142	< 0.001	$\omega0=0.022$, $\omega1=1.000$, $\omega2=1.000$	
		Alternative			$\omega0=0.022$, $\omega1=1.000$, $\omega2=645.215$	90 T 0.958*;179 P 1.000**;182 I 0.958*
	UCP1					
		Branch (terminal branch of *Heterocephalus glaber*)				
		Null	4.804	0.028	$\omega0=0.136$, $\omega1=1.000$, $\omega2=1.000$	
		Alternative			$\omega0=0.137$, $\omega1=1.000$, $\omega2=999.000$	166 P 0.934
Clade C	*HIF2A*					
		Pantholops hodgsonii and *Bos grunniens*				
		Clade C	7.276	0.007	$\omega0=0.017$, $\omega1=1.000$, $\omega2=0.291$, $\omega3=0.751$	
		M2a_rel			$\omega0=0.017$, $\omega1=1.000$, $\omega2=0.307$	
	PHD3					
		All cetaceans				
		Clade C	3.744	0.053	$\omega0=0.007$, $\omega1=1.000$, $\omega2=0.168$, $\omega3=1.162$	
		M2a_rel			$\omega0=0.014$, $\omega1=1.000$, $\omega2=0.441$	
	PGC-1					
		All cetaceans				
		Clade C	9.566	0.002	$\omega0=0.025$, $\omega1=1.000$, $\omega2=0.358$, $\omega3=1.554$	
		M2a_rel			$\omega0=0.000$, $\omega1=1.000$, $\omega2=0.207$	
		All pikas				
		Clade C	7.178	0.007	$\omega0=0.049$, $\omega1=1.000$, $\omega2=0.646$, $\omega3=4.214$	
		M2a_rel			$\omega0=0.000$, $\omega1=1.000$, $\omega2=0.207$	

sites in cetaceans and three sites in subterranean rodents) (Table S13, ESM). However, we did not detect any unique sites shared by pikas, Tibetan antelope and domestic yak native to high altitudes, which was probably because these mammals were distantly related in the phylogenetic tree.

Structures Linked to Protein Function

We mapped PSSs on the crystal structures of the corresponding genes to access the influence of selection on the structure and function of each gene (Figs. S8–S15, ESM). For 23 PSSs among five genes in the HIF pathway, three sites (584 in HIF1α, 468 in HIF2α and 262 in HIF1β) were located in or near functional domains. In HIF1α and HIF2α, these two sites were located within or near the ODDD/N-TAD domain (Table 2, Figs. S8–S9, ESM), and residue 262 in HIF1β was adjacent to the PER ARNT SIM A (PAS-A) domain (Table 2, Fig S10, ESM). For 24 PSSs in PGC-1 and UCP1, seven sites in PGC-1 (102, 205, 208, 224, 313, 634 and 698) were located within functional domains, and both residues 84 and 108 in UCP1 were close to sites whose mutation will impair nucleotide sensitivity of proton transport (Table 2, Figs. S14–S15, ESM) (Klingenspor et al. 2008). Among six sites in PGC-1, residues 102, 205, 208 and 224 were in the domains that can interact with the nuclear receptor (Knutti et al. 2000), 313 and 634 were located within the nuclear localization signal (NLS) domain and 698 was in the RNA binding (RNP) domain (Table 2, Fig. S15, ESM). In addition, in the pikas-only dataset, two sites with radical amino acid changes (326 and 714) in PGC-1 were located within the NLS domain and RNP domain, respectively (Table 1).

By mapping convergent/parallel and unique amino acid substitutions onto the 3D structures of the corresponding proteins, we aimed to illustrate how these sites

affected protein function. For genes in the HIF pathway, one convergent site (L/R439H in HIF2α) and two unique substitutions (578T in HIF1α and 451S in HIF2α) in diving cetaceans were distributed within the ODDD/N-TAD domain (Tables S12-S13, Figs. S8–S9, ESM). Moreover, a unique substitution (140S) in diving cetaceans was found to locate in the β2β3 loop of PHD3, which will participate in binding to target prolines (Table S13, Fig. S13, ESM) (Chowdhury et al. 2016).

Selective Pressure Analysis of Pseudogenized *UCP1* in Cetaceans

Based on the sequence alignment of *UCP1*, we identified premature stop codons located in the C-terminal region of all examined cetaceans. We analysed the selective pressure affecting cetaceans by removing the premature stop codons and then followed the procedures described in Zhao et al. (2010) to estimate ω using PAML. Based on a comparison between model A (one ratio) and model B (one ratio constrained), we found that the average ω across all mammals was 0.236 ($p < 0.001$), suggesting that purifying selection still played key roles in the evolution of *UCP1* to maintain its function in NST (Table 4). Then we constructed model C, which allowed a difference in ω between pseudogenized cetacean branches ($\omega = 1.780$) and all other branches ($\omega = 0.205$), to observe selective pressure on pseudogenized cetacean lineages. Based on the LRT test, model C fit the data better than model A ($p < 0.001$), indicating a different ω in cetaceans. Consistent with this result, model E, which allowed variant ω across the tree, was a significantly better fit than model C, suggesting that the selective pressure of each branch was different from one another ($p = 0.001$). Interestingly, model D, which had a fixed $\omega = 1$ in pseudogenized cetacean branches, was better than model C ($p = 0.098$), suggesting that functional constraints on cetaceans have already been completely removed.

Discussion

Adaptive Hypoxia and Cold Adaptation in Pikas

Pikas are small, non-hibernating lagomorphs native to high-altitude plateaus, where they experience chronic hypoxia and cold temperatures. In our study, three hypoxia responsive genes were positively selected, including *HIF1B, PHD2* and *PHD3* (Table 1). Particularly, positive signals in *PHD3* were detected by M2a and M8 in site model and at least REL and FUBAR methods in Datamonkey, which was indicative of strong adaptive evolution signals on *PHD3*. Further identification of sites with radical changes in amino acid properties in these three genes validated our conclusion. However, positive signals were not so strong in *HIF1A* or *HIF2A*, since both of them had only one PSS detected by FEL method alone (data not shown). Again, differential gene expression analysis did not reveal any gene up- or down-regulated between American pikas from high and low altitudes (Tables S7-S8, ESM).

Previous studies showed that pikas can rapidly adapt to cold stress under intermittent environmental cold exposure by "browning" white adipose tissues, which is achieved by increased expression of *UCP1* mainly in visceral adipose tissue (Bai et al. 2015). Furthermore, the NST content and UCP1 content in BAT were also significantly increased to enhance tolerance to cold temperatures in winter (Wang et al. 2006). Consistent with this finding, *UCP1* was shown to be positively selected in pikas with one PSS showing a radical change in its amino acid properties (Table 1). In addition, PGC-1, which can co-activate the transcriptional factors assembled on UCP1 (Lowell and Spiegelman 2000), had seven amino acid sites detected by M8 in site model and at least REL and FUBAR methods in Datamonkey (Table 1). Further protein mapping results suggested that two sites of PGC-1 were located within functional domains, including residue 326 in the NLS domain and 714 in the RNP domain. A previous study showed that the C-terminus containing the RNP domain contributed to the co-activation function of PGC-1 (Knutti et al. 2000). In addition, leptin,

Table 4 Likelihood ratio tests of various models on the selective pressures of *UCP1*

Models	ω values	-lnL	np	Model compared	2ΔLnL	*p*-value
All branches have one ω (A)	0.236	4494.304	52			
All branches have one $\omega = 1$ (B)	1.000	4677.101	51	B VS A	365.594	< 0.001
All cetacean branches have $\omega 2$, others have $\omega 1$ (C)	$\omega 1 = 0.205$ $\omega 2 = 1.780$	4472.137	53	A VS C	44.334	< 0.001
All cetacean branches have $\omega 2 = 1$, others have $\omega 1$ (D)	$\omega 1 = 0.205$ $\omega 2 = 1.000$	4473.508	52	D VS C	2.742	0.098
Each branch has its own ω (E)	Variable ω by branch	4430.548	101	C VS E	83.178	0.001

an adipocyte-derived hormone playing important roles in energy homeostasis, was also suggested to be positively selected in pikas and had a superior induced capacity for NST (Yang et al. 2008, 2011). Taken together, we proposed that adaptation to cold environments in pikas was driven by adaptive evolution, but the underlying mechanisms were complex and finely orchestrated by NST-related genes; further functional experiments are needed to clarify their relationships.

Molecular Evolution of the HIF Pathway in Hypoxia-Tolerant Mammals

In addition to high-altitude mammals that must survive in hypoxic environments, mammals occupying aquatic ecosystems and burrows with poor ventilation are also exposed to hypoxic conditions. Physiological adaptations that independently evolved in hypoxia-tolerant mammals have been intensively investigated, and they include but are not limited to modified circulatory and respiratory systems and enhanced O_2 carrying ability in the blood (Ge et al. 1998; Johansen et al. 1976; Maina et al. 2001; Panneton 2013; Qi et al. 2008; Ramirez et al. 2007). However, exploration of the molecular mechanisms underlying their hypoxia tolerance has only begun in recent decades. For example, genomic analysis in four marine mammals (the walrus (*Odobenus rosmarus*), bottlenose dolphin, killer whale (*Orcinus orca*) and manatee (*Trichechus manatus latirostris*)) revealed that parallel substitutions in positively selected genes may contribute to their cardiovascular regulation (*Myh7b*) and the low flow rate of viscous blood during diving (*Serpinc1*) (Foote et al. 2015). Using genomic data from indigenous people of the Tibetan Plateau, Hu et al. (2017) found that several positively selected genes were involved in high-altitude adaptation, and both *HIF2A* and *PHD2* were among top candidate genes. Here, we focused on six genes in the HIF pathway to conduct comparative analyses among representative hypoxia-tolerant mammals occupying high-altitude, aquatic and subterranean niches to explore the underlying mechanisms of hypoxia tolerance in different mammals.

In our study, all six genes except for *FIH-1* in the HIF pathway showed signals of positive selection with a total of 23 PSSs identified by at least two ML methods when the results from site model and Datamonkey were combined (Table 2). Of these 23, nine sites in three genes (*HIF1A, HIF2A* and *PHD3*) were demonstrated to have radical changes in amino acid properties, further validating our adaptive evolution signals. Moreover, three sites (584 in HIF1α, 468 in HIF2α and 262 in HIF1β) were located in or near functional domains (Table 2, Figs. S8–S10, ESM). In HIF1α and HIF2α, both sites were within or near the ODDD/N-TAD domain, which is responsible for the degradation and recruitment of transcriptional co-activators, whereas 262 in HIF1β was close to PAS-A domain which is involved in DNA binding and dimerization (Chowdhury et al. 2008). Interestingly, in PHD3, five PSSs (9, 16, 53, 55 and 234) were located within positions that were conserved within two of the three PHDs (PHD1-3); in particular, 16, the only site with radical amino acid changes, was shown to be conserved across all three PHDs. In addition, branch site model also suggested that the common bottlenose dolphin had two PSSs (179 P 1.000**; 182 I 0.958*) that were conserved across all three PHDs (Table 3). These changes might lead to the relaxation of PHD-dependent degradation of HIFα, thus contributing to adaptation to low O_2 conditions. However, their contribution to protein function still requires further functional verification; in this study, we have provided a series of candidate sites that may be helpful in future studies.

Based on results from branch site and Clade C model, which label a specific branch as the focal clade, we found that different hypoxia-tolerant mammal groups may prefer distinct components of the HIF pathway (Table 3). According to branch site model, only high-altitude Tibetan antelope was positively selected in *HIF2A* ($\omega 2 = 999.000$, $p < 0.001$). Interestingly, Clade C model also detected higher ω value falling on the clade containing domestic yak and Tibetan antelope ($\omega 2 = 0.291$, $\omega 3 = 0.751$, $p = 0.007$). In contrast, *PHD3* was positively selected in branches occupying two niches, including American pika ($\omega 2 = 67.825$, $p = 0.007$) and common bottlenose dolphin ($\omega 2 = 645.215$, $p < 0.001$), according to the branch site model. Furthermore, Clade C model revealed that the clade containing all cetaceans was marginally positively selected in *PHD3* ($\omega 3 = 1.162$, $p = 0.053$). And our differential gene expression analyses from lung and heart transcriptome data also revealed that *PHD3* was up-regulated in the heart of high-altitude domestic yak. In addition, previous studies also suggested that many target genes in the HIF pathway showed increased gene expression levels and/or significant adaptive evolution signals in above hypoxia-tolerant mammals (Fang et al. 2014a; Ge et al. 2013; Li et al. 2013; McGowen et al. 2012; Qiu et al. 2012; Schmidt et al. 2017). Hence, we proposed that the HIF pathway played important roles during mammalian adaptation to hypoxic conditions; however, it seemed that the mechanisms underlying independent mammalian invasions to hypoxic environments may differ.

Convergent and Unique Substitutions Contribute to Hypoxia Adaptation

Similar environmental challenges may induce convergent phenotypic adaptations between independently evolved species, and convergent evolution of a specific characteristic can arise from convergent/parallel amino acid replacements and/or unique substitutions; however, a key question in

evolutionary biology is to what extent a convergent phenotype is caused by such amino acid substitutions (Bridgham 2016; Natarajan et al. 2016; Stern 2013; Zhang and Kumar 1997). Independent invasions of high-altitude, subterranean and marine niches by different mammals provide a naturally occurring example to study convergent adaptation to hypoxic environments. Previous studies have already revealed a series of convergent physiological adaptations in hypoxia-tolerant mammals, such as modified circulatory and respiratory systems and enhanced O_2 carrying ability in the blood (Ge et al. 1998; Johansen et al. 1976; Maina et al. 2001; Panneton 2013; Qi et al. 2008; Ramirez et al. 2007). In our study, based on sequence alignments, we identified ten parallel/convergent sites occurred among hypoxia-tolerant mammals in the HIF pathway genes, and one convergent site (L/R439H in HIF2α between the naked mole rat and blind mole rat) was distributed within the ODDD/N-TAD domain (Table S12, ESM). However, based on comparison of observed and expected number of convergent/parallel substitutions among each pair of hypoxia-tolerant mammals under JTT-f_{site} model, our results revealed five pairs of hypoxia-tolerant mammals in four HIF pathway genes (including *HIF1A, HIF2A, HIF1B* and *PHD3*) which possessed significant higher-than-neutral substitutions (Table S11, ESM). Again, unlike the *prestin* gene, which grouped echolocation bats and dolphins together (Li et al. 2010; Liu et al. 2010), our phylogenetic reconstructions of each gene from the HIF pathway did not group any high-altitude, subterranean or diving mammals together (Figs. S2–S7, ESM). This result was not unpredictable, because responses to hypoxia challenges are controlled by many genes; thus, only the weak convergent effects detected in these genes were reasonable.

Since the convergent signals affecting the HIF pathway were week, we further investigated whether unique substitutions existed in different hypoxia-tolerant mammal groups (i.e. high-altitude, subterranean and diving groups). Finally, we identified 11 and three unique substitutions in diving cetaceans and subterranean rodents, respectively (Table S13, ESM). Moreover, among unique substitutions in cetaceans, 578T in HIF1α and 451S in HIF2α in diving cetaceans were distributed within the ODDD/N-TAD domain. In addition, 140S in PHD3 was within the β2β3 loop (Table S13, Fig. S13, ESM), which is a major determinant of NODD and CODD selectivity (Flashman et al. 2008). However, we did not detect any unique sites shared by pikas, Tibetan antelope and domestic yak native to high altitudes, which was likely due to the fact that these mammals are distantly related on the phylogenetic tree. Thus, we proposed that convergent and unique adjustments of the HIF pathway may coexist or separately play roles during independent invasions of high-altitude, subterranean and marine niches by different mammals based on our combined analyses of convergent sites within functional domains.

Different Molecular Mechanisms Underlying Adaptations to Fluctuant Temperatures in Mammals

Mammals in different niches will encounter divergent ambient temperatures. Animals living at high altitudes, such as pikas and domestic yaks, are challenged by consistently low temperatures; fully aquatic cetaceans face the high thermal conductivity and heat capacity of water, particularly in species that live in cold water. The burrow atmosphere of subterranean rodents that live underground features relatively constant temperatures compared to the outside temperature; for example, the burrow temperature of the naked mole rat is approximately 27 ~ 31 °C (Bennett et al. 1988). However, for blind mole rats living in the northern cool-humid Upper Galilee Mountains, which often became flooded (Nevo et al. 2001), it is difficult for their nest temperature to reach a thermoneutral zone. Placental mammals can increase their heat production in cold temperatures by NST-mediated *UCP1* expression in BAT; in particular, *UCP1* expression can reach 5% of the total mitochondrial protein content in cold acclimated rodents (Stuart et al. 2001). Based on investigation in vertebrates, Klingenspor et al. (2008) detected an accelerated evolution of *UCP1* in placental mammal lineages; however, Hughes et al. (2009) suggested that the increased ω value on the branch leading to Eutherians should be best explained by relaxed constraints, not positive selection. However, in our analyses, based on molecular evolution analyses of *UCP1* and its co-activator *PGC-1* in the all-mammals datasets (for *UCP1*, all cetaceans were removed), our study provided three lines of evidence to support the positive signals affecting placental mammals. First, 24 PSSs were identified by at least two ML methods in Datamonkey, including two sites in *UCP1* and 22 sites in *PGC-1* (Table 2). Second, 12 PSSs in *PGC-1* had radical changes in their amino acid properties. Furthermore, four positively selected sites (102, 205, 208 and 224) in PGC-1 were located within the nuclear receptor interaction domain 1 and 2 (NID1 and 2) (Table 2, Fig. S15, ESM), and their deletion will eliminate PGC-1 activity (Knutti et al. 2000). In addition, two positively selected sites 84 and 108 in UCP1 were close to sites whose mutation will impair nucleotide sensitivity of proton transport (Klingenspor et al. 2008). Additionally, branch site model also revealed that naked mole rat was positively selected and residue Trp166 was positively selected under BEB analysis (Table 3). Trp166 was among the putative GDP binding sites, whose mutation may influence the GDP-sensitive fatty acid inducible proton leak in UCP1 (Klingenspor et al. 2008). This finding was consistent with previous genomic analysis conducted by Kim et al. (2011). Third, Clade C model revealed that in *PGC-1* positive selection was located on two focal clades, all cetaceans ($\omega 3 = 1.554$, $p = 0.002$) and all pikas ($\omega 3 = 4.214$, $p = 0.007$) (Table 3), which were all exposed to low temperatures.

As diving mammals, cetaceans evolved a thick blubber layer to defend against heat loss in the water, only leaving a thermal window within peripheral sites (dorsal fins and flukes) to transfer excess heat (Kanwisher and Ridgway 1983; McGinnis et al. 1972; Ryg et al. 1993), and vessels in peripheral sites were arranged in a counter-current manner (Hampton and Whittow 1976; Scholander and Schevill 1955). Peripheral vasoconstriction occurred and heat flow declined in both the dorsal fin and flank when the animals dove, further reducing heat loss to the water (Skrovan et al. 1999). Investigations of the common bottlenose dolphin showed that their skin temperature often remained within 1 °C of the water temperature (Noren et al. 1999). Thus, we proposed that these adaptations in aquatic cetaceans may eliminate their need for high levels of heat production. In favour of this hypothesis, we identified premature stop codons within the C-terminal region of *UCP1* in all examined cetaceans, which was consistent with genomic analysis in the bowhead whale (Keane et al. 2015). Further selective pressure analysis also suggested that functional constraints were almost completely removed from cetaceans (Table 4), indicating that the loss of *UCP1* may have occurred immediately after their divergence from cloven-hoofed partners. Interestingly, pigs, another member of Cetartiodactyla, were also shown to have a pseudogenized *UCP1* due to the deletion of exons 3–5, and the disruption of *UCP1* may have occurred approximately 20 million years ago (Berg et al. 2006). Since modern cetaceans originated approximately 34 million years ago (Thewissen et al. 2009; Zhou et al. 2011), we thus proposed that the loss of *UCP1* may have occurred independently in pig and cetaceans. However, a previous study identified the existence of BAT in cetacean blubber through the immunohistochemical positive reaction specific to UCP1 in four species of delphinoid cetaceans (Hashimoto et al. 2015), creating ambiguity about the existence of UCP1 in cetaceans. Hence, we assumed that *UCP1* may have evolved a new function or continue to perform its original function in a weaker form, but further functional experiments are still needed to clarify this.

Conclusion

In this study, genes playing important roles in NST and the HIF pathway were investigated in pikas and other hypoxia-tolerant mammals. Selective pressure analyses showed that during the evolution of pikas, natural selection may have been a primary driving force in their adaptation to hypoxia and cold environments. Further analyses in the HIF pathway genes revealed pervasive positive selection signals and weak convergent effects in mammals occupying divergent hypoxic niches. *UCP1* and *PGC-1*, which participate in cold adaptation, also showed strong positive selection signals in high-altitude and subterranean mammals; however, *UCP1* may have lost its function in cetaceans, which may be related to their insulating blubber. In addition, it should be noted that functional estimates based on ω cannot replace physiological and biochemical studies and that additional integrative approaches at molecular, physiology, biochemistry and genomics levels are required to fully understand these mechanisms. Our analyses provide a series of functionally important candidate sites for future functional experiments.

Acknowledgements This work was supported by Key Laboratory of Zoological Systematics and Evolution of the Chinese Academy of Sciences (No. Y229YX5105) and National Special Fund on Basic Research of Science and Technology of China (No. 2014FY110100). The authors wish to thank the members of our lab for collecting samples for so many years.

References

Arieli R, Heth G, Nevo E, Hoch D (1986) Hematocrit and hemoglobin concentration in four chromosomal species and some isolated populations of actively speciating subterranean mole rats in Israel. Experientia 42:441–443

Bai ZZ, Tana WR, Liu S, Han SR, Chen L, McClain D, Ge RL (2015) Intermittent cold exposure results in visceral adipose tissue "browning" in the plateau pika (*Ochotona curzoniae*). Comp Biochem Physiol A Mol Integr Physiol 184:171–178

Bennett NC, Jarvis JUM, Davies KC (1988) Daily and seasonal temperatures in the burrows of African rodent moles. S Afr J Zool 23:189–195

Berg F, Gustafson U, Andersson L (2006) The uncoupling protein 1 gene (*UCP1*) is disrupted in the pig lineage: a genetic explanation for poor thermoregulation in piglets. PLos Genet 2:e129

Bi JL, Hu B, Zheng JS, Wang JZ, Xiao WH, Wang D (2015) Characterization of the hypoxia-inducible factor 1 alpha gene in the sperm whale, beluga whale, and Yangtze finless porpoise. Mar Biol 162:1201–1213

Bolger AM, Lohse M, Usadel B (2014) Trimmomatic: a flexible trimmer for Illumina sequence data. Bioinformatics 30:2114–2120

Bouillaud F, Weissenbach J, Ricquier D (1986) Complete cDNA-derived amino acid sequence of rat brown fat uncoupling protein. J Biol Chem 261:1487–1490

Bridgham JT (2016) Predicting the basis of convergent evolution. Science 354:289–289

Buffenstein R (2000) Ecophysiological responses of subterranean rodents to underground habitats. In: Lacey EA, Patton JL, Cameron GN (eds), Life underground, the biology of subterranean rodents, University Chicago Press, Chicago, pp 62–110

Cannon B, Nedergaard J (2004) Brown adipose tissue: Function and physiological significance. Physiol Rev 84:277–359

Castresana J (2000) Selection of conserved blocks from multiple alignments for their use in phylogenetic analysis. Mol Biol Evol 17:540–552

Chowdhury R, Hardy A, Schofield CJ (2008) The human oxygen sensing machinery and its manipulation. Chem Soc Rev 37:1308–1319

Chowdhury R, Leung IKH, Tian Y-M, Abboud MI, Ge W, Domene C, Cantrelle F-X, Landrieu I, Hardy AP, Pugh CW, Ratcliffe PJ, Claridge TDW, Schofield CJ (2016) Structural basis for oxygen degradation domain selectivity of the HIF prolyl hydroxylases. Nat Commun 7:12673

Citta JJ, Suydam RS, Quakenbush LT, Frost KJ, O'Corry-Crowe GM (2013) Dive behavior of eastern chukchi beluga whales (*Delphinapterus leucas*), 1998–2008. Arctic 66:389–406

Corbet GB (1978) The mammals of the palaearctic region: a taxonomic review. British Museum (Natural History) and Cornell University Press, London

Darriba D, Taboada GL, Doallo R, Posada D (2012) jModelTest 2: more models, new heuristics and parallel computing. Nat Methods 9:772–772

Dobin A, Davis CA, Schlesinger F, Drenkow J, Zaleski C, Jha S, Batut P, Chaisson M, Gingeras TR (2013) STAR: ultrafast universal RNA-seq aligner. Bioinformatics 29:15–21

Dunkin RC, McLellan WA, Blum JE, Pabst DA (2005) The ontogenetic changes in the thermal properties of blubber from Atlantic bottlenose dolphin *Tursiops truncatus*. J Exp Biol 208:1469–1480

Enerbäck S, Jacobsson A, Simpson EM, Guerra C, Yamashita H, Harper M-E, Kozak LP (1997) Mice lacking mitochondrial uncoupling protein are cold-sensitive but not obese. Nature 387:90–94

Fang X, Nevo E, Han L, Levanon EY, Zhao J, Avivi A, Larkin D, Jiang X, Feranchuk S, Zhu Y, Fishman A, Feng Y, Sher N, Xiong Z, Hankeln T, Huang Z, Gorbunova V, Zhang L, Zhao W, Wildman DE, Xiong Y, Gudkov A, Zheng Q, Rechavi G, Liu S, Bazak L, Chen J, Knisbacher BA, Lu Y, Shams I, Gajda K, Farré M, Kim J, Lewin HA, Ma J, Band M, Bicker A, Kranz A, Mattheus T, Schmidt H, Seluanov A, Azpurua J, McGowen MR, Ben Jacob E, Li K, Peng S, Zhu X, Liao X, Li S, Krogh A, Zhou X, Brodsky L, Wang J (2014a) Genome-wide adaptive complexes to underground stresses in blind mole rats Spalax. Nat Commun 5:3966

Fang X, Seim I, Huang Z, Gerashchenko Maxim V, Xiong Z, Turanov Anton A, Zhu Y, Lobanov Alexei V, Fan D, Yim Sun H, Yao X, Ma S, Yang L, Lee SG, Kim Eun B, Bronson Roderick T, Šumbera R, Buffenstein R, Zhou X, Krogh A, Park Thomas J, Zhang G, Wang J, Gladyshev Vadim N (2014b) Adaptations to a subterranean environment and longevity revealed by the analysis of mole rat genomes. Cell Rep 8:1354–1364

Flashman E, Bagg EAL, Chowdhury R, Mecinović J, Loenarz C, McDonough MA, Hewitson KS, Schofield CJ (2008) Kinetic rationale for selectivity toward N- and C-terminal oxygen-dependent degradation domain substrates mediated by a loop region of hypoxia-inducible factor prolyl hydroxylases. J Biol Chem 283:3808–3815

Foote AD, Liu Y, Thomas GWC, Vinař T, Alföldi J, Deng J, Dugan S, van Elk CE, Hunter ME, Joshi V, Khan Z, Kovar C, Lee SL, Lindblad-Toh K, Mancia A, Nielsen R, Qin X, Qu J, Raney BJ, Vijay N, Wolf JBW, Hahn MW, Muzny DM, Worley KC, Gilbert MTP, Gibbs RA (2015) Convergent evolution of the genomes of marine mammals. Nat Genet 47:272–275

Ge RL, Kubo K, Kobayashi T, Sekiguchi M, Honda T (1998) Blunted hypoxic pulmonary vasoconstrictive response in the rodent *Ochotona curzoniae* (pika) at high altitude. Am J Physiol 274:H1792–H1799

Ge DY, Zhang ZQ, Xia L, Zhang Q, Ma Y, Yang QS (2012) Did the expansion of C4 plants drive extinction and massive range contraction of micromammals? Inferences from food preference and historical biogeography of pikas. Palaeogeogr Palaeoclimatol Palaeoecol 326–328:160–171

Ge RL, Cai Q, Shen Y-Y, San A, Ma L, Zhang Y, Yi X, Chen Y, Yang L, Huang Y, He R, Hui Y, Hao M, Li Y, Wang B, Ou X, Xu J, Zhang Y, Wu K, Geng C, Zhou W, Zhou T, Irwin DM, Yang Y, Ying L, Bao H, Kim J, Larkin DM, Ma J, Lewin HA, Xing J, Platt RN, Ray DA, Auvil L, Capitanu B, Zhang X, Zhang G, Murphy RW, Wang J, Zhang Y-P, Wang J (2013) Draft genome sequence of the Tibetan antelope. Nat Commun 4:1858

Gompel N, Prud'homme B (2009) The causes of repeated genetic evolution. Dev Biol 332:36–47

Guindon S, Gascuel O, Rannala B (2003) A simple, fast, and accurate algorithm to estimate large phylogenies by maximum likelihood. Syst Biol 52:696–704

Hampton IF, Whittow GC (1976) Body temperature and heat exchange in the Hawaiian spinner dolphin, *Stenella longirostris*. Comp Biochem Physiol A Comp Physiol 55:195–197

Hashimoto O, Ohtsuki H, Kakizaki T, Amou K, Sato R, Doi S, Kobayashi S, Matsuda A, Sugiyama M, Funaba M, Matsuishi T, Terasawa F, Shindo J, Endo H (2015) Brown Adipose tissue in cetacean blubber. PLos One 10:e0116734

Hoffmann RS (1993) Order lagomorpha. In: Wilson DE, Reeder DM (eds) Mammalian species of the world, a taxonomic and geographic reference. Smithsonian Institution Press, Washington, pp 807–827

Hu H, Petousi N, Glusman G, Yu Y, Bohlender R, Tashi T, Downie JM, Roach JC, Cole AM, Lorenzo FR, Rogers AR, Brunkow ME, Cavalleri G, Hood L, Alpatty SM, Prchal JT, Jorde LB, Robbins PA, Simonson TS, Huff CD (2017) Evolutionary history of Tibetans inferred from whole-genome sequencing. PLos Genet 13:e1006675

Hughes DA, Jastroch M, Stoneking M, Klingenspor M (2009) Molecular evolution of UCP1 and the evolutionary history of mammalian non-shivering thermogenesis. BMC Evol Biol 9:4

Jacobsson A, Stadler U, Glotzer MA, Kozak LP (1985) Mitochondrial uncoupling protein from mouse brown fat. Molecular cloning, genetic mapping, and mRNA expression. J Biol Chem 260:16250–16254

Johansen K, Lykkeboe G, Weber RE, Maloiy GM (1976) Blood respiratory properties in the naked mole rat *Heterocephalus glaber*, a mammal of low body temperature. Respir Physiol 28:303–314

Kanwisher JW, Ridgway SH (1983) The physiological ecology of whales and porpoises. Sci Am 248:110–120

Keane M, Semeiks J, Webb AE, Li YI, Quesada V, Craig T, Madsen LB, van DS, Brawand, Marques D, Michalak PI, Kang P, Bhak L, Yim J, Grishin H-S, Nielsen NV, Heide-Jørgensen NH, Oziolor MP, Matson EM, Church CW, Stuart GM, Patton GW, George JC, Suydam JC, Larsen R, López-Otín K, O'Connell C, Bickham MJ, Thomsen JW, de Magalhães B JP (2015) Insights into the evolution of longevity from the bowhead whale genome. Cell Rep 10:112–122

Kim EB, Fang XD, Fushan AA, Huang ZY, Lobanov AV, Han LJ, Marino SM, Sun XQ, Turanov AA, Yang PC, Yim SH, Zhao X, Kasaikina MV, Stoletzki N, Peng CF, Polak P, Xiong ZQ, Kiezun A, Zhu YB, Chen YX, Kryukov GV, Zhang Q, Peshkin L, Yang L, Bronson RT, Buffenstein R, Wang B, Han CL, Li QY, Chen L, Zhao W, Sunyaev SR, Park TJ, Zhang GJ, Wang J, Gladyshev VN (2011) Genome sequencing reveals insights into physiology and longevity of the naked mole rat. Nature 479:223–227

Kim D, Pertea G, Trapnell C, Pimentel H, Kelley R, Salzberg SL (2013) TopHat2: accurate alignment of transcriptomes in the presence of insertions, deletions and gene fusions. Genome Biol 14:R36

Klingenberg M, Huang SG (1999) Structure and function of the uncoupling protein from brown adipose tissue. Biochim Biophys Acta 1415:271–296

Klingenspor M, Fromme T, Hughes DA, Manzke L, Polymeropoulos E, Riemann T, Trzcionka M, Hirschberg V, Jastroch M (2008) An ancient look at UCP1. Biochim Biophys Acta 1777:637–641

Knutti D, Kaul A, Kralli A (2000) A tissue-specific coactivator of steroid receptors, identified in a functional genetic screen. Mol Cell Biol 20:2411–2422

Kosakovsky Pond SL, Frost SD (2005a) Datamonkey: rapid detection of selective pressure on individual sites of codon alignments. Bioinformatics 21:2531–2533

Kosakovsky Pond SL, Frost SD (2005b) Not so different after all: a comparison of methods for detecting amino acid sites under selection. Mol Biol Evol 22:1208–1222

Kovacs KM, Lydersen C, Overland JE, Moore SE (2011) Impacts of changing sea-ice conditions on Arctic marine mammals. Mar Biodiv 41:181–194

Langmead B, Salzberg SL (2012) Fast gapped-read alignment with Bowtie 2. Nat Methods 9:357–359

Law CW, Chen Y, Shi W, Smyth GK (2014) voom: precision weights unlock linear model analysis tools for RNA-seq read counts. Genome Biol 15:R29

Lemay MA, Henry P, Lamb CT, Robson KM, Russello MA (2013) Novel genomic resources for a climate change sensitive mammal: characterization of the American pika transcriptome. BMC Genom 14:311

Li B, Dewey CN (2011) RSEM: accurate transcript quantification from RNA-Seq data with or without a reference genome. BMC Bioinf 12:323

Li Q, Sun R, Huang C, Wang Z, Liu X, Hou J, Liu J, Cai L, Li N, Zhang S, Wang Y (2001) Cold adaptive thermogenesis in small mammals from different geographical zones of China. Comp Biochem Physiol A Mol Integr Physiol 129:949–961

Li HG, Ren YM, Guo SC, Cheng L, Wang DP, Yang J, Chang ZJ, Zhao XQ (2009) The protein level of hypoxia-inducible Factor-1 alpha is increased in the Plateau Pika (*Ochotona curzoniae*) inhabiting high altitudes. J Exp Zool A Ecol Genet Physiol 311:134–141

Li Y, Liu Z, Shi P, Zhang JZ (2010) The hearing gene Prestin unites echolocating bats and whales. Curr Biol 20:R55–R56

Li H, Guo S, Ren Y, Wang D, Yu H, Li W, Zhao X, Chang Z (2013) VEGF189 expression is highly related to adaptation of the Plateau Pika (*Ochotona curzoniae*) inhabiting high altitudes. High Alt Med Biol 14:395–404

Liao Y, Smyth GK, Shi W (2014) Feature counts: an efficient general purpose program for assigning sequence reads to genomic features. Bioinformatics 30:923–930

Lindblad-Toh K, Garber M, Zuk O, Lin MF, Parker BJ, Washietl S, Kheradpour P, Ernst J, Jordan G, Mauceli E, Ward LD, Lowe CB, Holloway AK, Clamp M, Gnerre S, Alföldi J, Beal K, Chang J, Clawson H, Cuff J, Di Palma F, Fitzgerald S, Flicek P, Guttman M, Hubisz MJ, Jaffe DB, Jungreis I, Kent WJ, Kostka D, Lara M, Martins AL, Massingham T, Moltke I, Raney BJ, Rasmussen MD, Robinson J, Stark A, Vilella AJ, Wen J, Xie X, Zody MC, Baldwin J, Bloom T, Whye Chin C, Heiman D, Nicol R, Nusbaum C, Young S, Wilkinson J, Worley KC, Kovar CL, Muzny DM, Gibbs RA, Cree A, Dihn HH, Fowler G, Jhangiani S, Joshi V, Lee S, Lewis LR, Nazareth LV, Okwuonu G, Santibanez J, Warren WC, Mardis ER, Weinstock GM, Wilson RK, Delehaunty K, Dooling D, Fronik C, Fulton L, Fulton B, Graves T, Minx P, Sodergren E, Birney E, Margulies EH, Herrero J, Green ED, Haussler D, Siepel A, Goldman N, Pollard KS, Pedersen JS, Lander ES, Kellis M (2011) A high-resolution map of human evolutionary constraint using 29 mammals. Nature 478:476–482

Liu Y, Cotton JA, Shen B, Han X, Rossiter SJ, Zhang S (2010) Convergent sequence evolution between echolocating bats and dolphins. Curr Biol 20:R53–R54

Losos JB (2011) Convergence, adaptation, and constraint. Evolution 65:1827–1840

Lowell BB, Spiegelman BM (2000) Towards a molecular understanding of adaptive thermogenesis. Nature 404:652–660

Maina JN, Gebreegziabher Y, Woodley R, Buffenstein R (2001) Effects of change in environmental temperature and natural shifts in carbon dioxide and oxygen concentrations on the lungs of captive naked mole-rats (*Heterocephalus glaber*): a morphological and morphometric study. J Zool Lond 253:371–382

Masson N, Ratcliffe PJ (2014) Hypoxia signaling pathways in cancer metabolism: the importance of co-selecting interconnected physiological pathways. Cancer Metab 2:3

Maxwell PH (2005) Hypoxia-inducible factor as a physiological regulator. Exp Physiol 90:791–797

McGinnis SM, Whittow GC, Ohata CA, Huber H (1972) Body heat dissipation and conservation in two species of dolphins. Comp Biochem Physiol A Comp Physiol 43:417–423

McGowen MR, Grossman LI, Wildman DE (2012) Dolphin genome provides evidence for adaptive evolution of nervous system genes and a molecular rate slowdown. Proc Biol Sci 279:3643–3651

Merkin J, Russell C, Chen P, Burge CB (2012) Evolutionary dynamics of gene and isoform regulation in mammalian tissues. Science 338:1593–1595

Murrell B, Moola S, Mabona A, Weighill T, Sheward D, Kosakovsky Pond SL, Scheffler K (2013) FUBAR: a fast, unconstrained bayesian approximation for inferring selection. Mol Biol Evol 30:1196–1205

Natarajan C, Projecto-Garcia J, Moriyama H, Weber RE, Muñoz-Fuentes V, Green AJ, Kopuchian C, Tubaro PL, Alza L, Bulgarella M, Smith MM, Wilson RE, Fago A, McCracken KG, Storz JF (2015) Convergent evolution of hemoglobin function in high-altitude andean waterfowl involves limited parallelism at the molecular sequence level. Plos Genet 11:e1005681

Natarajan C, Hoffmann FG, Weber RE, Fago A, Witt CC, Storz JF (2016) Predictable convergence in hemoglobin function has unpredictable molecular underpinnings. Science 354:336–339

Nevo E, Ivanitskaya E, Beiles A (2001) Adaptive radiation of blind subterranean mole rats: naming and revisiting the four sibling species of the Spalax ehrenbergi superspecies in Israel: *Spalax galili* (2n = 52), *S. golani* (2n = 54), S. *carmeli* (2n = 58), and *S. judaei* (2n = 60). Backhuys, Kerkwerve

Nicholls DG, Locke RM (1984) Thermogenic mechanisms in brown fat. Physiol Rev 64:1–64

Noren DP, Williams TM, Berry P, Butler E (1999) Thermoregulation during swimming and diving in bottlenose dolphins, *Tursiops truncatus*. J Comp Physiol B 169:93–99

Panneton WM (2013) The Mammalian diving response: an enigmatic reflex to preserve life? Physiology 28:284–297

Parsons PA (2005) Environments and evolution: interactions between stress, resource inadequacy and energetic efficiency. Biol Rev 80:589–610

Pichon A, Zhenzhong B, Marchant D, Jin G, Voituron N, Haixia Y, Favret F, Richalet JP, Ge RL (2013) Cardiac adaptation to high altitude in the plateau pika (*Ochotona curzoniae*). Physiol Rep 1:e00032

Puigserver P, Wu Z, Park CW, Graves R, Wright M, Spiegelman BM (1998) A cold-inducible coactivator of nuclear receptors linked to adaptive thermogenesis. Cell 92:829–839

Qi XZ, Wang XJ, Zhu SH, Rao XF, Wei L, Wei DB (2008) Hypoxic adaptation of the hearts of plateau zokor (*Myospalax baileyi*) and plateau pika (*Ochotona curzoniae*). Acta Physiol Sin 60:348–354

Qiu Q, Zhang GJ, Ma T, Qian WB, Wang JY, Ye ZQ, Cao CC, Hu QJ, Kim J, Larkin DM, Auvil L, Capitanu B, Ma J, Lewin HA, Qian XJ, Lang YS, Zhou R, Wang LZ, Wang K, Xia JQ, Liao SG, Pan SK, Lu X, Hou HL, Wang Y, Zang XT, Yin Y, Ma H, Zhang J, Wang ZF, Zhang YM, Zhang DW, Yonezawa T, Hasegawa M, Zhong Y, Liu WB, Zhang Y, Huang ZY, Zhang SX, Long RJ, Yang HM, Wang J, Lenstra JA, Cooper DN, Wu Y, Wang J, Shi P, Wang J, Liu JQ (2012) The yak genome and adaptation to life at high altitude. Nat Genet 44:946–949

Ramirez JM, Folkow LP, Blix AS (2007) Hypoxia tolerance in mammals and birds: from the wilderness to the clinic. Annu Rev Physiol 69:113–143

Robinson MD, Oshlack A (2010) A scaling normalization method for differential expression analysis of RNA-seq data. Genome Biol 11:R25

Robinson MD, McCarthy DJ, Smyth GK (2009) edgeR: a Bioconductor package for differential expression analysis of digital gene expression data. Bioinformatics 26:139–140

Ronquist F, Teslenko M, van der Mark P, Ayres DL, Darling A, Höhna S, Larget B, Liu L, Suchard MA, Huelsenbeck JP (2012) MrBayes 3.2: efficient bayesian phylogenetic inference and model choice across a large model space. Syst Biol 61:539–542

Ryg M, Lydersen C, Knutsen LO, Bjorge A, Smith TG, Oritsland NA (1993) Scaling of insulation in seals and whales. J Zool Lond 230:193–206

Schmidt H, Malik A, Bicker A, Poetzsch G, Avivi A, Shams I, Hankeln T (2017) Hypoxia tolerance, longevity and cancer-resistance in the mole rat Spalax—a liver transcriptomics approach. Sci Rep 7:14348

Scholander PF, Schevill WE (1955) Counter-current vascular heat exchange in the fins of whales. J Appl Physiol 8:279–282

Shams I, Avivi A, Nevo E (2004) Hypoxic stress tolerance of the blind subterranean mole rat: expression of erythropoietin and hypoxia-inducible factor 1. Proc Natl Acad Sci 101:9698–9703

Sheafor BA (2003) Metabolic enzyme activities across an altitudinal gradient: an examination of pikas (genus Ochotona). J Exp Biol 206:1241–1249

Skrovan RC, Williams TM, Berry PS, Moore PW, Davis RW (1999) The diving physiology of bottlenose dolphins (*Tursiops truncatus*)—II. Biomechanics and changes in buoyancy at depth. J Exp Biol 202:2749–2761

Stern DL (2013) The genetic causes of convergent evolution. Nat Rev Genet 14:751–764

Stern DL, Orgogozo V (2009) Is genetic evolution predictable? Science 323:746–751

Storz JF (2016) Causes of molecular convergence and parallelism in protein evolution. Nat Rev Genet 17:239–250

Struntz DJ, McLellan WA, Dillaman RM, Blum JE, Kucklick JR, Pabst DA (2004) Blubber development in bottlenose dolphins (*Tursiops truncatus*). J Morphol 259:7–20

Stuart JA, Harper JA, Brindle KM, Jekabsons MB, Brand MD (2001) A mitochondrial uncoupling artifact can be caused by expression of uncoupling protein 1 in yeast. Biochem J 356:779–789

Sunagar K, Johnson WE, O'Brien SJ, Vasconcelos V, Antunes A (2012) Evolution of CRISPs associated with toxicoferan-reptilian venom and mammalian reproduction. Mol Biol Evol 29:1807–1822

Suzuki Y, Nei M (2002) Simulation study of the reliability and robustness of the statistical methods for detecting positive selection at single amino acid sites. Mol Biol Evol 19:1865–1869

Suzuki Y, Nei M (2004) False-positive selection identified by ML-based methods: examples from the Sig1 gene of the diatom *Thalassiosira weissflogii* and the tax gene of a human T-cell lymphotropic virus. Mol Biol Evol 21:914–921

Tamura K, Stecher G, Peterson D, Filipski A, Kumar S (2013) MEGA6: molecular evolutionary genetics analysis version 6.0. Mol Biol Evol 30:2725–2729

Thewissen JGM, Cooper LN, George JC, Bajpai S (2009) From land to water: the origin of whales, dolphins, and porpoises. Evoluat Edu Outreach 2:272–288

Thompson JD, Higgins DG, Gibson TJ (1994) CLUSTAL W: improving the sensitivity of progressive multiple sequence alignment through sequence weighting, position-specific gap penalties and weight matrix choice. Nucl Acid Res 22:4673–4680

Wang JM, Zhang YM, Wang DH (2006) Seasonal thermogenesis and body mass regulation in plateau pikas (*Ochotona curzoniae*). Oecologia 149:373–382

Woolley S, Johnson J, Smith MJ, Crandall KA, McClellan DA (2003) TreeSAAP: selection on amino acid properties using phylogenetic trees. Bioinformatics 19:671–672

Yang Z (2005) Bayes empirical bayes inference of amino acid sites under positive selection. Mol Biol Evol 22:1107–1118

Yang Z (2007) PAML 4: phylogenetic analysis by maximum likelihood. Mol Biol Evol 24:1586–1591

Yang ZH, dos Reis M (2011) Statistical properties of the branch-site test of positive selection. Mol Biol Evol 28:1217–1228

Yang ZH, Nielsen R, Goldman N, Pedersen AMK (2000) Codon-substitution models for heterogeneous selection pressure at amino acid sites. Genetics 155:431–449

Yang J, Wang ZL, Zhao XQ, Wang de P, Qi de L, Xu BH, Ren YH, Tian HF (2008) Natural selection and adaptive evolution of leptin in the ochotona family driven by the cold environmental stress. PLos One 3:e1472

Yang J, Bromage TG, Zhao Q, Xu BH, Gao WL, Tian HF, Tang HJ, Liu DW, Zhao XQ (2011) Functional evolution of leptin of *Ochotona curzoniae* in adaptive thermogenesis driven by cold environmental stress. PLos One 6:e19833

Yim HS, Cho YS, Guang X, Kang SG, Jeong JY, Cha SS, Oh HM, Lee JH, Yang EC, Kwon KK, Kim YJ, Kim TW, Kim W, Jeon JH, Kim SJ, Choi DH, Jho S, Kim HM, Ko J, Kim H, Shin YA, Jung HJ, Zheng Y, Wang Z, Chen Y, Chen M, Jiang A, Li E, Zhang S, Hou H, Kim TH, Yu L, Liu S, Ahn K, Cooper J, Park SG, Hong CP, Jin W, Kim HS, Park C, Lee K, Chun S, Morin PA, O'Brien SJ, Lee H, Kimura J, Moon DY, Manica A, Edwards J, Kim BC, Kim S, Wang J, Bhak J, Lee HS, Lee JH (2014) Minke whale genome and aquatic adaptation in cetaceans. Nat Genet 46:88–92

Zhang Y (2008) I-TASSER server for protein 3D structure prediction. BMC Bioinformatics 9:40

Zhang J, Kumar S (1997) Detection of convergent and parallel evolution at the amino acid sequence level. Mol Biol Evol 14:527–536

Zhang N, Fu Z, Linke S, Chicher J, Gorman JJ, Visk D, Haddad GG, Poellinger L, Peet DJ, Powell F, Johnson RS (2010) The asparaginyl hydroxylase factor inhibiting HIF-1alpha is an essential regulator of metabolism. Cell Metab 11:364–378

Zhao H, Yang JR, Xu H, Zhang J (2010) Pseudogenization of the umami taste receptor gene Tas1r1 in the giant panda coincided with its dietary switch to bamboo. Mol Biol Evol 27:2669–2673

Zhou X, Xu S, Yang Y, Zhou K, Yang G (2011) Phylogenomic analyses and improved resolution of Cetartiodactyla. Mol Phylogenet Evol 61:255–264

Zou Z, Zhang J (2015) Are convergent and parallel amino acid substitutions in protein evolution more prevalent than neutral expectations? Mol Biol Evol 32:2085–2096